Antiviral Research 160 (2018) 126–136

Contents lists available at ScienceDirect

Antiviral Research

journal homepage: www.elsevier.com/locate/antiviral

MNK1 inhibitor as an antiviral agent suppresses buffalopox virus protein synthesis

Ram Kumar[a,b,1], Nitin Khandelwal[a,1], Yogesh Chander[a,1], Thachamvally Riyesh[a], Bhupendra N. Tripathi[a], Sudhir Kumar Kashyap[b], Sanjay Barua[a,**], Sunil Maherchandani[b,***], Naveen Kumar[a,*]

[a] National Centre for Veterinary Type Cultures, ICAR-National Research Centre on Equines, Hisar, India
[b] Department of Veterinary Microbiology and Biotechnology, Rajasthan University of Veterinary and Animal Sciences, Bikaner, India

ARTICLE INFO

Keywords:
MNK1
CGP57380
Antiviral efficacy
Protein synthesis
Drug resistance

ABSTRACT

A small molecule chemical inhibitor CGP57380 that blocks activation of MAPK interacting kinase 1 (MNK1) was found to significantly suppress buffalopox virus (BPXV) replication. BPXV infection was shown to induce MNK1 activation. Depletion of MNK1 by small interfering RNA (siRNA), blocking activation of extracellular regulated kinase (ERK, an upstream activator of MNK1) and disruption of eIF4E/eIF4G interaction (downstream substrate of MNK1 which plays a central role in cap-dependent translation initiation), resulted in reduced BPXV replication, suggesting that ERK/MNK1/eIF4E signaling is a prerequisite for BPXV replication. With the help of time-of-addition and virus step-specific assays, CGP57380 treatment was shown to decrease synthesis of viral genome (DNA). Disruption of ERK/MNK1/eIF4E signaling resulted in reduced synthesis of viral proteins, suggesting that BPXV utilizes cap-dependent mechanism of translation initiation. Therefore, we concluded that decreased synthesis of viral genome in presence of MNK1 inhibitor is the result of reduced synthesis of viral proteins. Furthermore, BPXV was sequentially passaged (P = 40) in presence of CGP57380 or vehicle control (DMSO). As compared to P0 and P40-control viruses, P40-CGP57380 virus replicated at significantly higher (~10-fold) titers in presence of CGP57380, although a complete resistance could not be achieved. In a BPXV egg infection model, CGP57380 was found to prevent development of pock lesions on chorioallantoic membrane (CAM) as well as associated mortality of the embryonated chicken eggs. We for the first time demonstrated *in vitro* and *in ovo* antiviral efficacy of CGP57380 against BPXV and identified that ERK/MNK1 signaling is a prerequisite for synthesis of viral proteins. Our study also describes a rare report about generation of drug-resistant viral variants against a host-targeting antiviral agent.

1. Introduction

Buffalopox is caused by an orthopoxvirus that belongs to the family *Poxviridae*. The natural host for buffalopox virus (BPXV) is domestic buffalo (*Bubalus bubalis*), but it can also infect cattle and humans and hence is considered as a potential zoonotic threat (Gujarati et al., 2018; Lewis-Jones, 2004; Singh et al., 2006, 2007). Buffalopox outbreaks have been reported in India, Egypt, Indonesia and Italy (Gujarati et al., 2018; Marinaik et al., 2018; Singh et al., 2007). Buffalopox virus (BPXV) infection in humans have been frequently reported in India (Bera et al., 2012; Dumbell and Richardson, 1993; Gujarati et al., 2018; Gurav et al., 2011; Marinaik et al., 2018; Riyesh et al., 2014; Singh et al., 2006).

Buffalopox is characterized by development of pustular skin lesions, which may be localized or disseminated, depending upon the disease severity. Disease outbreaks in buffaloes often result in decreased milk production (Singh et al., 2007; Venkatesan et al., 2010). To minimize the economic impact, blocking virus transmission during epidemics is of utmost importance for which rapid control tools are urgently required (Goris et al., 2008). Despite adverse effect on animal industry and severe consequences to human health (Singh et al., 2007), antiviral drugs that can be used to treat buffalopox or other viral infections of

* Corresponding author.
** Corresponding author.
*** Corresponding author.
E-mail addresses: sbarua06@gmail.com (S. Barua), smchandani86@gmail.com (S. Maherchandani), naveenkumar.icar@gmail.com (N. Kumar).
[1] Equal contribution.

https://doi.org/10.1016/j.antiviral.2018.10.022
Received 14 July 2018; Received in revised form 22 October 2018; Accepted 24 October 2018
Available online 28 October 2018

animals are lacking.

Most of the antiviral agents that are licensed for use are based on directly targeting viral components (Chen et al., 2016). High mutation rate in viral genome allows the virus to become resistant at the druggable targets (Andino and Domingo, 2015). This rise in incidence of drug resistance has prompted a paradigm shift in the approaches for the development of antiviral drugs (Ludwig et al., 2006). Upon viral infection, an array of signal transduction events are initiated by the cells that are basically antiviral (Kumar et al., 2016b; Ludwig et al., 2006). However, there are evidences that the virus has acquired the capability to exploit host cell signaling pathways to support its effective replication (Kumar et al., 2011, 2018b; Muhlbauer et al., 2015; Pleschka et al., 2001). Number of such studies are in preclinical development and will ultimately lead to the definition of specific cellular targets for novel antiviral approaches. Compared to the high rate of mutations in viral genome, genetic variability of the host is quite low and hence host-targeting agents are considered to impose a higher genetic barrier to generation of resistant viruses. Therefore, a potential good approach for development of novel antiviral therapeutics is to target host factors required for efficient virus replication.

Protein phosphorylation and dephosphorylation, mediated respectively via kinase and phosphatase, is a ubiquitous cellular regulatory mechanism during signal transduction which determines key cellular processes such as growth, development, transcription, metabolism, apoptosis, immune response, and cell differentiation. Kinome-the protein kinase complement of the human genome, completed in 2002, identified 518 protein kinase genes. These kinases have been shown to play a key role in cancer and many other diseases (Coito et al., 2004) including viral infections (Nousiainen et al., 2013), making these proteins very desirable drug targets. We reviewed the literature (Boss et al., 2009; Cinats et al., 2018; Glover et al., 2004; Hartmann et al., 2009; Schoffski et al., 2006; Wang et al., 2011) and selected some kinase inhibitors that are commercially available. One of the inhibitor (CGP57380) that inhibits activation of MAPK interacting kinase 1 (MNK1) by blocking its phosphorylation (Grzmil et al., 2014; Huang et al., 2018; Knauf et al., 2001; Martinez et al., 2015; Shveygert et al., 2010) was shown to impair BPXV replication in cultured Vero cells. In this study, we evaluated *in vitro* and *in ovo* antiviral efficacy of MNK1 inhibitor against BPXV and identified that MNK1 is a critical cellular factor required for synthesis of viral proteins. We also studied the potential development of drug-resistant BPXV variants on long-term passage in presence of MNK1 inhibitor (a host-targeting antiviral agent).

2. Materials and methods

2.1. Chemicals

MNK1 inhibitor- CGP57380 (Fig. 1), Extracellular regulated kinase (ERK) inhibitor- FR180204, MTT [3-(4,5-dimethyl-2-thiazolyl)-2,5-diphenyl-2H-tetrazolium bromide] and dimethyl sulfoxide (DMSO) were procured from Sigma (Steinheim, Germany) whereas eIF4E/eIF4G interaction inhibitor 4EGI-1 was procured from EMD Millipore (Darmstadt, Germany).

2.2. Cell culture

African green monkey kidney (Vero) and HeLa cells were available at National Centre for Veterinary Type Cultures (NCVTC), Hisar. Cells were grown in Minimum Essential Medium (MEM) supplemented with 10% fetal bovine serum (FBS) (Sigma, St. Louis, USA) and antibiotics.

2.3. BPXV

Cell culture adapted BPXV (Accession Number, VTCC-AVA90) was available at NCVTC Hisar, which was amplified and quantitated by plaque assay in Vero cells. Briefly, Vero cells were grown in 6 well tissue culture plates. The confluent monolayers were infected with 10-fold serial dilutions (in 500 µl volume) of the virus for 1 h at 37 °C, after which the infecting medium was removed and replaced with agar-overlay containing equal volume of 2X L-15 medium and 2% agar. The plaques were visible at 5–6 days post infection (dpi) after which agar-overlay was removed and the plaques were stained by crystal violet (1% crystal violet and 20% methanol). The viral titers were determined as plaque forming unit/ml (pfu/ml).

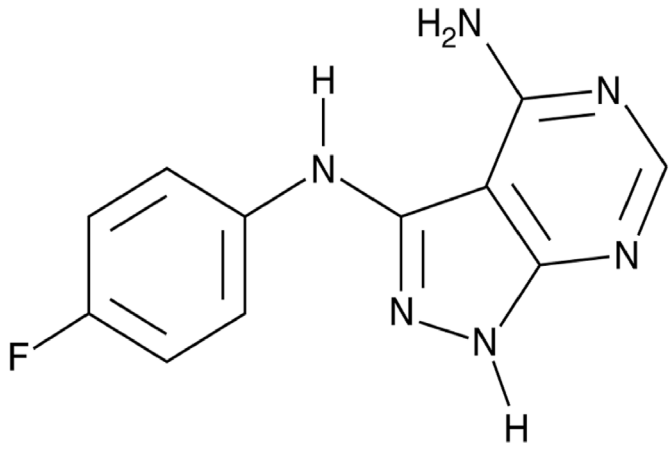

Fig. 1. CGP57380 (MNK1 inhibitor): N^3-(4-Fluorophenyl)-1H-pyrazolo-[3,4-d] pyrimidine-3,4-diamine).

2.4. Evaluation of MNK1 activation following BPXV infection

HeLa cells were infected with BPXV at MOI of 5 in 30 cm tissue culture dishes. Cell lysates were prepared at 1 h post infection (hpi), 6 hpi, 12 hpi, 18 hpi and at 24 hpi, and subjected for detection of phosphorylated MNK1 (pMNK1) in Western blot analysis by using a phospho-specific MNK1antibody [(RbmAb to MNK1 phospho T 385 (Abcam, Cambridge, USA) and Goat Anti-Rabbit IgG HRP conjugate (Sigma, St. Louis, USA). Total MNK1 was detected using Rabbit MNK1 Polyclonal Antibody (Thermo Fisher Scientific, Rockford, USA). The house-keeping control protein [Glyceraldehyde 3-phosphate dehydrogenase (GAPDH)] was probed using Mouse anti-GAPDH primary antibody (Sigma, St. Louis, USA) and Anti-Mouse IgG (whole molecule)-Alkaline Phosphatase conjugate (Sigma, St. Louis, USA).

2.5. Cytotoxicity and virucidal activity

The cytotoxic (Kumar et al., 2008) and virucidal effects (Kumar et al., 2011) of CGP57380 were determined as previously described.

2.6. In vitro antiviral efficacy of CGP57380 (EC_{50})

Vero cells, in triplicates were infected with BPXV at MOI of 0.1 for 1 h followed by washing with PBS, and addition of fresh MEM containing either DMSO or 5-fold serial dilutions of the CGP57380 (8 µg/ml to 0.064 µg/ml). Viral titers in the infected cell culture supernatants at 48 hpi were determined by plaque assay. Effective concentration 50 (EC_{50}, concentration of the inhibitor required to reduce 50% virus yield) was determined by Reed-Muench method.

2.7. Effect of MNK1 inhibitor on specific steps of BPXV life cycle

2.7.1. Time-of-addition assay

Confluent monolayers of Vero cells, in triplicates were infected with BPXV at MOI of 5, followed by addition of CGP57380 (1.5 µg/ml) or vehicle-control at 1 hpi, 6 hpi, 12 hpi, 18 hpi, 24 hpi, 30 hpi and 36 hpi. Supernatant from the infected cells was collected at 48 hpi and

quantified by plaque assay.

2.7.2. Attachment assay

Confluent monolayers of Vero cells, in triplicates, were pre-incubated with 1.5 μg/ml CGP57380 or 0.05% DMSO for 30 min followed by BPXV infection at MOI of 5 for 2 h at 4 °C. The cells were then washed 5 times with PBS and the cell lysates were prepared by rapid freeze-thaw method. The viral titers in cell lysates were quantified by plaque assay.

2.7.3. Entry assay

Confluent monolayers of Vero cells, in triplicates, were pre-chilled at 4 °C and infected with BPXV at MOI of 5 in CGP57380-free medium for 1.5 h at 4 °C, which allowed virus attachment to the host cells but restricted viral entry. Thereafter, the cells were washed with PBS and incubated with fresh MEM containing 1.5 μg/ml CGP57380 or 0.05% DMSO. To permit viral entry, cells were incubated at 37 °C for 1 h. Thereafter, cells were washed with PBS and grown in fresh MEM without any inhibitor. Virus yield in the infected cell culture supernatants at 48 hpi was determined by plaque assay.

2.7.4. Virus release assay

Confluent monolayers of Vero cells, in triplicates, were infected with BPXV at MOI of 5 for 1 h. Thereafter, cells were washed with PBS and fresh MEM was added. At 36 hpi, cells were washed 5 times with chilled PBS followed by addition of fresh MEM containing 1.5 μg/ml CGP57380 or vehicle-control. Virus yield in infected cell culture supernatant at 30 min and 4 h post-drug treatment was quantified by plaque assay.

2.7.5. qRT-PCR

The amounts of viral DNA in infected cells were measured by quantitative real-time PCR (qRT-PCR). Confluent monolayers of Vero cells, in triplicates, were infected with BPXV (MOI of 5) for 1 h followed by washing with PBS and addition of fresh MEM. CGP57380 (1.5 μg/ml) or DMSO (0.05%) were added at 6 hpi. Cells were scraped at 36 hpi to quantify the viral (C18L) and house-keeping control gene (β-actin) by qRT-PCR as previously described (Khandelwal et al., 2017). The levels of viral DNA, expressed as threshold cycle (*Ct*) values, were normalized with β-actin housekeeping control gene. Relative fold-change in viral DNA copy number was determined by ΔΔ Ct method (Kumar et al., 2016a).

2.7.6. Effect of CGP57380 on synthesis of viral proteins

Confluent monolayers of Vero cells were grown in 30 cm^2 tissue culture dishes and infected with BPXV at MOI of 5. Inhibitors or vehicle-control were added at 6 hpi. Cells were scraped at 36 hpi to analyze the levels of viral and house-keeping control protein (GAPDH) in Western blot. Anti-BPXV serum was available at NCVTC Hisar and has been described elsewhere (Khandelwal et al., 2017).

2.8. siRNA knockdown of MNK1

In order to further confirm the role of MNK1 in BPXV replication, as well as to avoid the possibilities that MNK1 inhibitor may have some off-target effects in the host cells, MNK1 was knockdown from the cells in a sequence dependent manner by using small interfering RNA (siRNA). Briefly, HeLa cells were grown in 96 well plates. When the cells were at ~75% confluency, 5 pmol of MNK1 [(MISSION siRNA Human Kinase MNK1 (siRNA4 nanoscale)] or control siRNA (MISSION siRNA Universal Negative Control) were transfected using Lipofectamine 3000 as per the instruction of manufacturer (Invitrogen, Carlsbad, USA). At 48 h post-transfection, cells were infected with BPXV at MOI of 1 and virus released in the infected cell culture supernatant at 48 hpi was quantified by plaque assay.

2.9. Selection of potential CGP57380-resistant virus variants

Vero cells were infected with BPXV at MOI of 0.1 in medium containing 0.05% DMSO or 0.5 μg/ml CGP57380. At 48–72 hpi, supernatant was collected from the virus infected cells [named passage 1 (P1)] and quantified by plaque assay. Forty such sequential passages were carried out. The original virus stock (P0), P40-CGP57380 and P40-control viruses were used to infect Vero cells at an MOI of 0.1 with either 1.5 μg/ml CGP57380 or 0.05% DMSO. At 48 hpi, viral titers in the infected cell culture supernatant were quantified by plaque assay.

2.10. In ovo antiviral efficacy of CGP57380 against BPXV

2.10.1. Egg lethal dose 50 (LD_{50})

Specific pathogen free (SPF) embryonated chicken eggs were procured from Indovax Pvt. Ltd., Hisar, India. LD_{50} of CGP57380 was determined by inoculating 5-fold serial dilutions of CGP57380 (concentration ranging from 500 to 0.16 μg/egg) or DMSO (vehicle-control), in 10 day old embryonated SPF eggs, in a total of 100 μl volumes via chorioallantoic membrane (CAM) route. Eggs were examined for the viability of the embryos up to five days post-inoculation to determine the LD_{50} by the Reed-Muench method.

2.10.2. Egg infective dose 50 (EID_{50})

EID_{50} of BPXV was determined by inoculating 100 μl of serial 10-fold dilutions of BPXV [stock of 10^7 pfu/ml], in 10 day old embryonated SPF eggs via CAM route. At 5 dpi, eggs were visualized for pock lesions on its CAM. For determining EID_{50}, development of pock lesions on CAM and/or death of the embryos were considered as mortality.

2.10.3. In ovo antiviral efficacy (EC_{50})

SPF embryonated chicken eggs, in triplicates, were inoculated with 5-fold dilutions (25–0.1 μg/egg) of CGP57380 or equal volume of vehicle control via CAM route, followed by infection with BPXV at 100 EID_{50}. On 5–7 dpi, eggs were examined for pock lesions and/or death of the embryos. EC_{50} was determined by the Reed-Muench method.

3. Results

3.1. In vitro antiviral efficacy of CGP57380

The cytotoxicity of CGP57380 was determined by MTT assay. To estimate the viability, Vero cells were grown in the presence of five-fold increasing concentrations (up to 40 μM) of CGP57380 for 72 hpi. As shown in Fig. 2a, no significant cytotoxicity in Vero cells was observed up to 1.6 μg/ml. A marginal cell death (~10%) was observed at 8 μg/ml and a significant (~50%) cell death was observed at 40 μg/ml. The CC_{50} was determined to be 38.03 μg/ml (Reed-Muench method).

To determine the antiviral efficacy, virus yields in BPXV-infected Vero cells were measured in presence of indicated concentrations of CGP57380 or equivalent volume of vehicle-control. As compared to the vehicle-control, CGP57380 significantly inhibited BPXV replication in a dose-dependent manner (~3 log at 8 μg/ml, ~2 log at 1.6 μg/ml and ~1 log at 0.32 μg/ml) (Fig. 2b) suggesting MNK1 supports BPXV replication. The EC_{50} was determined to be 0.075 μg/ml (Reed-Muench method).

To analyze the virucidal effects of CGP57380 on extracellular virions, BPXV was incubated with indicated concentrations of CGP57380 for 1.5 h and then titrated on Vero cells. As shown in Fig. 2c, infectious virus titers were comparable in both CGP57380 or vehicle control-treated aliquots, suggesting that CGP57380 exerts no direct virucidal effect on BPXV and that the antiviral efficacy of MNK1 inhibitor is presumably due to disruption of viral life cycle.

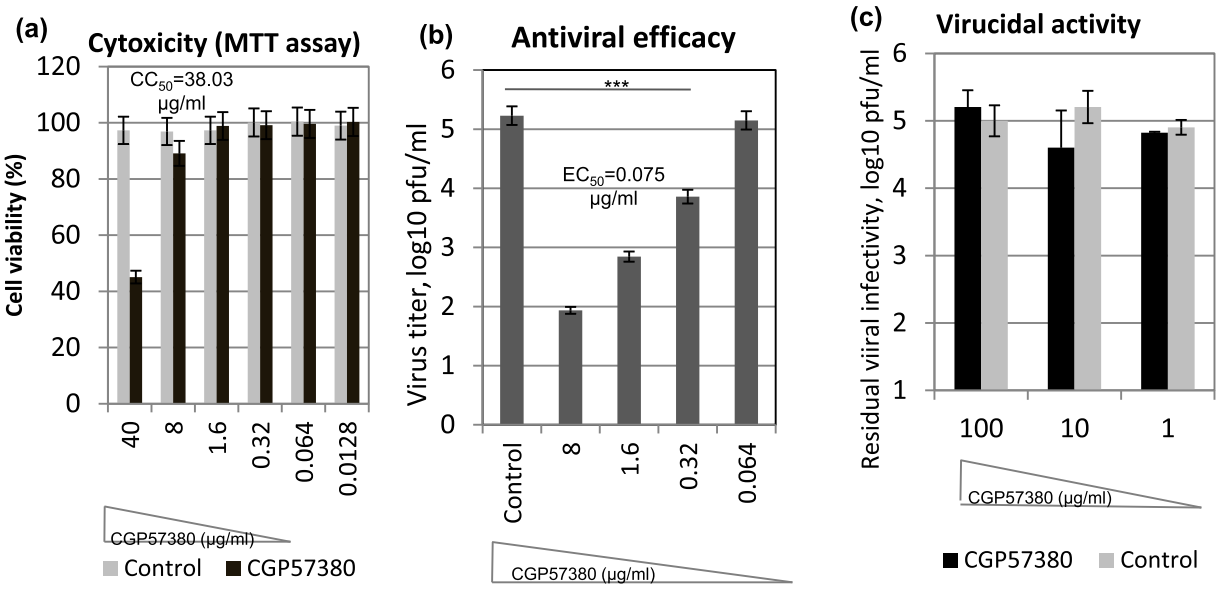

Fig. 2. *In vitro* antiviral efficacy of CGP57380. (a) *Cytotoxicity:* Indicated concentrations of CGP57380 or equivalent volumes of DMSO were incubated with cultured Vero cells for 96 h followed by measuring the cell viability (% survival) by MTT assay. ***(b) In vitro antiviral efficacy:*** Vero cells were infected with BPXV at MOI of 0.1 in the presence of indicated concentrations of CGP57380 or vehicle-control. The virus yield in the infected cell culture supernatants was quantified by plaque assay. Virus titers between vehicle control and various drug regimens were compared. Error bars indicate SD. Pair-wise statistical comparisons were performed using Student's *t*-test (*** = $P < 0.001$). ***(c) Virucidal activity:*** Indicated concentrations of the CGP57380 or equivalent volumes of DMSO were mixed with BPXV and incubated for 1.5 h at 37 °C, after which virus was diluted (1/1000) and relative infectivity was analyzed by plaque assay. CC_{50} and EC_{50} were determined by Reed-Muench method.

3.2. Time-of-addition assay

In order to estimate which step(s) of BPXV life cycle may be affected by CGP57380, a time-of-addition assay was performed in the setting of one-step growth curve. Vero cells were infected with BPXV and the inhibitor- or vehicle-controls were applied at different time post-infection (1 hpi to 36 hpi). When one full cycle of the BPXV was about to complete, i.e. at 36–48 hpi (Khandelwal et al., 2017), the infectious virus released in the infected cell culture supernatant was quantified. As shown in Fig. 3, application of CGP57380 resulted in a similar level of BPXV inhibition either applied before infection (pre-treatment) or at 1 hpi, 6 hpi, 12 hpi and 18 hpi, suggesting CGP57380 may not inhibit early step of BPXV life cycle. Addition of inhibitor at later time points showed low (at 24 hpi and 30 hpi) or no inhibition (36 hpi), suggesting that CGP57380 has no significant effect on late stage of BPXV life cycle.

3.3. BPXV infection induces MNK1 activation

Phosphorylated MNK1 (pMNK1) which serves as its marker of activation could be consistently detected at 1 hpi, 6 hpi, 12 hpi, 18 hpi and 24 hpi in BPXV-infected cells but not in mock-infected cells, suggesting that BPXV induces MNK1 activation. There was only a small amount of pMNK1 at 1 hpi (Fig. 4a). It peaked at 12 hpi and persisted till 18 hpi, after which it started declining at 24 hpi (Fig. 4a). Effect of BPXV was also examined on level of cellular house-keeping proteins (GAPDH) (Fig. 4b). No significant difference was observed in the GAPDH levels of mock-infected and BPXV-infected cells (Fig. 4b). Same cell lysate was also used to evaluate levels of total MNK1 (Fig. 4c) and GAPDH levels (Fig. 4d) wherein no significant changes were observed between different treatments suggesting that alteration in pMNK1 levels were due to BPXV infection, rather than an alteration in total MNK1 levels.

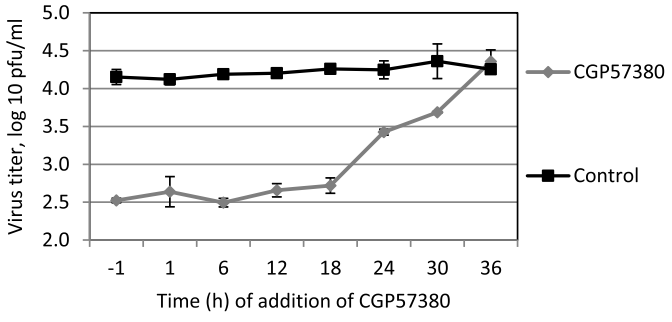

Fig. 3. Time-of-addition assay: Pre-treated (1.5 µg/ml of CGP57380) or non-treated Vero cells were infected, in triplicate with BPXV for 1 h followed by washing with PBS and addition of fresh MEM. Inhibitor or vehicle control was applied at indicated time points. Supernatants were collected at 48 h post-infection (hpi) and quantified by plaque assay.

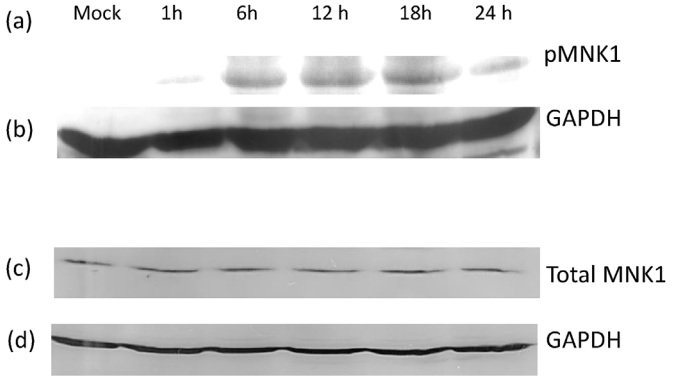

Fig. 4. BPXV induces MNK1 activation. HeLa cells were either mock-infected or infected with BPXV at MOI of 5. Cell lysate were prepared at indicated time points and subjected for Western blot analysis. First gel was run to detect the levels of pMNK1 (a) and GAPDH (b) whereas second gel (same cell lysate) was run to detect levels of total MNK1 (c) and GAPDH (d).

3.4. Effect of CGP57380 on attachment, entry and budding of BPXV

In order to determine the effect of CGP57380 on attachment of

BPXV to the host cells, virus infection was carried out at 4 °C which allowed virus attachment (adsorption) to the host cells but restricted viral entry. Viral titers were comparable in both vehicle-control-treated and CGP57380-treated cells suggesting that MNK1 inhibitor does not affect BPXV attachment to the host cells (Supplementary Fig. 1a).

To evaluate the effect of CGP57380 on BPXV entry, virus was first allowed to attach at 4 °C in absence of any inhibitor, followed by incubating the cells at 37 °C for 1 h (to permit viral entry) in presence of the inhibitor. Virus titers were comparable in both vehicle-control-treated and CGP57380-treated cells suggesting that MNK1 inhibitor does not affect BPXV entry into the target cells (Supplementary Fig. 1b).

It was also examined whether CGP57380 inhibits release of BPXV from infected cells. In virus release assay, the inhibitor was applied at the time when early (attachment/entry) and middle steps (genome and protein synthesis) of the viral life cycle had occurred and when virus presumably started budding from the infected cells i. e. at 36 hpi. Virus titers were comparable in both vehicle-control-treated and CGP57380-treated cells suggesting MNK1 inhibitor does not affect BPXV release from the infected cells (Supplementary Fig. 1c).

3.5. MNK1 regulates cap-dependent translation initiation of BPXV proteins

In order to determine the effect of CGP57380 on synthesis of BPXV genome, Vero cells were infected with BPXV and the inhibitor was applied at 6 hpi, a time point when early steps of the viral replication cycles are expected to occur. The cells were scrapped at 24 hpi to quantitate viral (C18L) and cellular (β-actin) genes by qRT-PCR. As compared to the vehicle-control-treated cells, CGP57380-treated cells showed ~66-fold reduction in viral DNA (Fig. 5a), suggesting that MNK1 inhibitor affects BPXV genome synthesis.

Since reduced viral DNA synthesis may eventually reflect reduction in synthesis of the viral proteins, levels of viral protein in inhibitor-treated and vehicle-treated cells were also examined. As shown in Fig. 5b (upper panel), CGP57380-treatment also resulted in decreased synthesis of viral proteins in infected cells whereas levels of house-keeping control protein GAPDH were unaffected (Fig. 5b, lower panel). Concomitant to the viral protein synthesis, a reduced amount of viral mRNA was also observed in inhibitor-treated cells (Fig. 5c).

Alternatively, it is possible that CGP57380 treatment might have resulted in reduced synthesis of viral polymerase which in turn would have resulted in reduced synthesis of viral genome. Viral mRNA translation in most of the DNA viruses (including poxviruses) and some RNA viruses is synthesized in cap-dependent manner where eIF4E/eIF4G interaction plays a central role in translation initiation. By binding to eIF4G, activated MNK1 may directly activate elF4E to initiate 5′-cap-dependent translation initiation. In order to evaluate whether BPXV utilize cap-dependent mechanism of translation initiation, we measured the yields of infectious virions in the supernatant of virus infected cells in presence of eIF4E/eIF4G interaction inhibitor-4EGI-1. At a noncytotoxic concentration of 5 μg/ml (Fig. 6a), 4EGI-1-treated cells produced significantly less virus, as compared to the control-treated cells (Fig. 6b), suggesting that BPXV utilizes cap-dependent mechanism of translation initiation. Therefore, blocking MNK1 activation that regulates eIF4E/eIF4G interaction, results in decreased BPXV production. Further, when we measured the levels of viral proteins; as compared to the control-treated cells, 4EGI-1-treated cells showed significantly lower amount of viral proteins (Fig. 6c) suggesting that MNK1 regulates BPXV protein synthesis and that decreased synthesis of BPXV genome in presence of CGP57380 is due to reduced synthesis of viral proteins.

Further, MNK1 was depleted from the HeLa cells by transfecting MNK1 siRNA. A reduced yield of infectious virus in MNK1 siRNA-treated cells, as compared to the control-siRNA treated cells further confirmed that MNK1 is a prerequisite for BPXV replication (Fig. 7a). Furthermore, ERK activation (an upstream regulator of MNK1) was blocked in cultured Vero cells using an ERK-specific chemical inhibitor FR180204. At a noncytotoxic concentration (1.0 μg/ml), (Fig. 7b), FR180204-treated cells showed a highly significant reduction (~3 log) in BPXV replication suggesting prerequisite of ERK/MNK1 signaling in BPXV replication.

3.6. Selection of drug resistant virus variants

To evaluate the generation of potential drug-resistant BPXV variants, BPXV was passaged 40 times in presence of MNK1 inhibitor (CGP57380, a host targeting agent) or vehicle control. Initially (P0) we

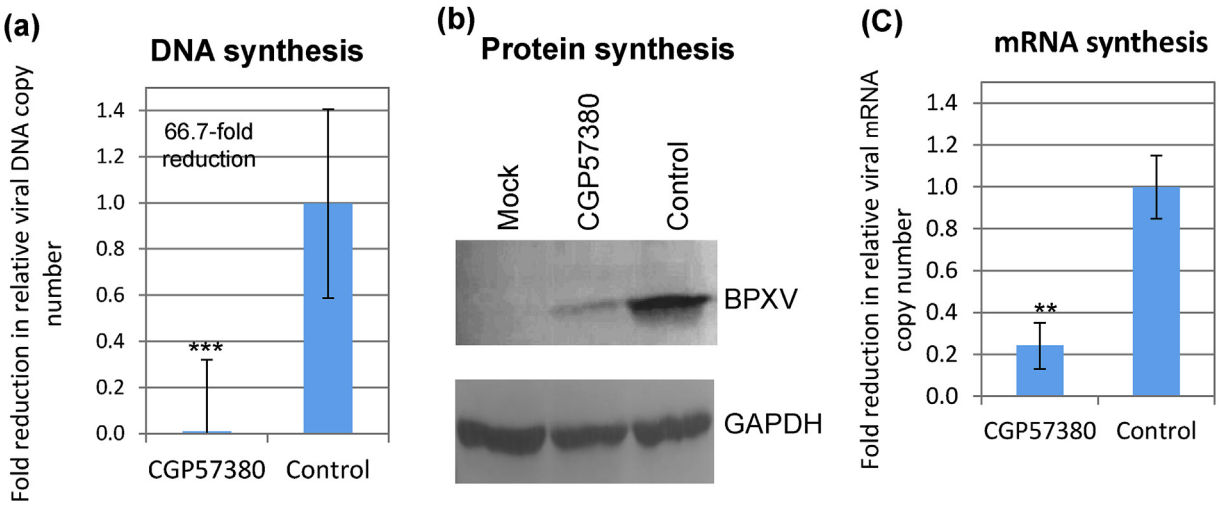

Fig. 5. Treatment of MNK1 inhibitor results in reduced synthesis of viral DNA/mRNA/proteins. Confluent monolayers of Vero cells were infected with BPXV (MOI of 5) for 1 h followed by washing with PBS and addition of fresh MEM. Inhibitor or vehicle-control was applied at 6 hpi. Cells were scraped at 36 hpi to quantify viral genome/proteins/mRNA. **(a)** Quantitation of BPXV C18L gene in CGP57380-treated and vehicle-control-treated Vero cells by qRT-PCR. Ct values were normalized with β-actin house-keeping control gene and relative fold change was calculated by ΔΔ Ct method. Graphical representation of the fold-change in relative copy number of viral DNA. **(b)** The levels of viral (upper panel) and GAPDH house-keeping control protein (lower panel) were determined by Western blot analysis. **(c)** Confluent monolayers of Vero cells were infected with BPXV at MOI of 5. Inhibitor or vehicle-control was applied at 6 hpi. Cells were scraped at 18 hpi to isolate total RNA, followed by cDNA preparation using oligo(dT) primers. The levels of BPXV mRNA (cDNA) in inhibitor-treated and untreated cells were quantified by qRT-PCR. Error bars indicate SD. Pair-wise statistical comparisons were performed using Student's t-test (** = $P < 0.01$, *** = $P < 0.001$).

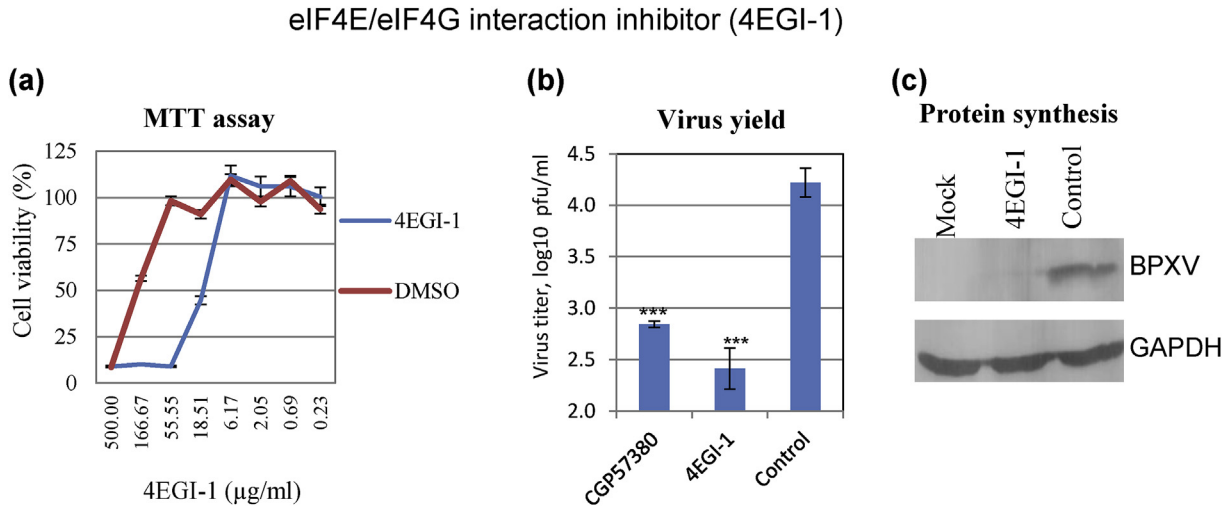

Fig. 6. Cap-dependent translation initiation of BPXV proteins. ***(a) Cytotoxicity of 4EGI-1:*** Indicated concentrations of eIF4E/eIF4G interaction inhibitor (4EGI-1) or equivalent volumes of DMSO were incubated with cultured Vero cells for 96 h and cell viability (% survival) was measured by MTT assay. **(b) Effect of *4EGI-1 on production of infectious BPXV in cultured cells:*** Vero cells were infected with BPXV at MOI of 1 in the presence of 5 µg/ml of 4EGI-1 or 0.05% DMSO. The virus yield in the infected cell culture supernatant was quantified by plaque assay. ***(c)*** **Effect of *4EGI-1 on synthesis of viral proteins.*** Vero cells were infected with BPXV at MOI of 1 in the presence of 5 µg/ml 4EGI-1 or 0.05% DMSO. Cell lysates were prepared at 36 hpi to quantify viral protein. (c) Error bars indicate SD. Pair-wise statistical comparisons were performed using Student's *t*-test (*** = P < 0.001).

observed ~500-fold inhibition in the viral titres in CGP57380-treated cells, as compared to the vehicle control (DMSO)-treated cells (Fig. 8a). The inhibition levels in viral titres were comparable even up to passage level 20 (P20) (Fig. 8a). However, later on, the viral inhibition levels progressively decreased i. e. ~10-fold inhibition at P40, as compared to ~500-fold inhibition at P0 (Fig. 8a). Fluctuations in the overall viral titres and hence variation in fold inhibition was observed (Fig. 8a), which might be due to the fact that the harvest time (72–96 h) and MOI (0.01–0.001) used was not similar at each passage. Therefore, we carried out an experiment wherein a similar MOI (MOI = 0.1) and harvest time (48 h) was used to evaluate the relative resistance in CGP57380-passaged and control-passaged viruses.

When the relative fitness was compared in presence of CGP57380, P40-CGP57380 virus was found to replicate at significantly higher (~10-fold) titres than P0 or P40-control viruses (Fig. 8b and c), suggesting acquisition of drug resistance by CGP57380-passaged virus. P40-control virus did not exhibit any significant resistance against CGP57380 even up to P40 (Fig. 8b) suggesting that resistance against CGP57380 is not a general phenomenon due to sequential high passages but rather a specific event acquired in presence of CGP57380.

In absence of any drug, P40-Control and P40-CGP57380 viruses replicated with similar viral titers (Fig. 8b), although, as compared to P0, they replicated at significantly higher titers (~8-fold) (Fig. 8b). In addition, as compared to the P0 virus, P40-Control and P40-CGP57380 viruses also produced plaques of slightly bigger size (Fig. 8d). These evidences suggested that sequential high passage of BPXV in cell culture would have resulted in some non-specific mutations (irrespective of the drug treatment) that enabled to replicate P40-Control and P40-CGP57380 viruses more efficiently and thereby producing bigger plaque sizes.

In order to further ascertain whether the resistance acquired by P40-CGP57380 virus was specifically directed against CGP57380 and not against any other antiviral agent, we evaluated the growth of P0, P40-Control and P40-CGP57380 viruses in presence of emetine, an antiviral

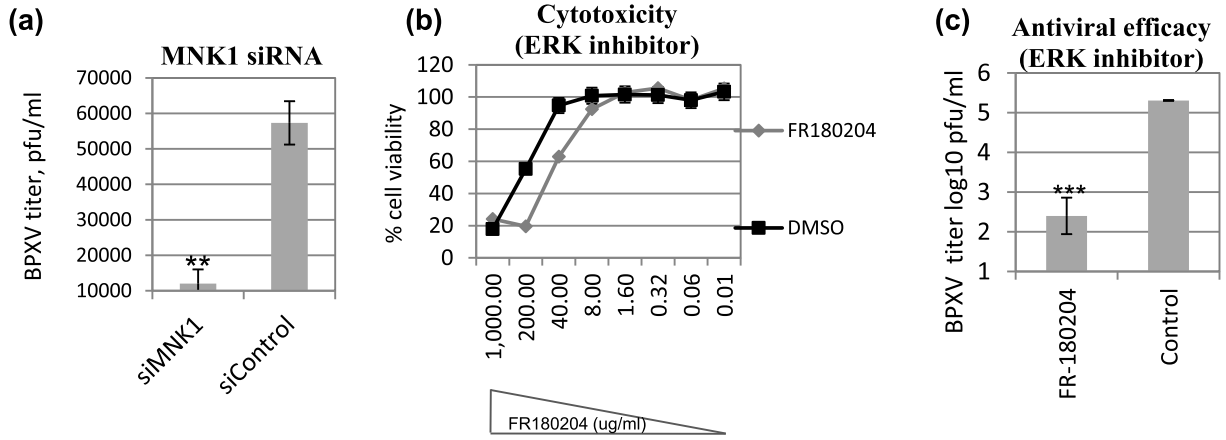

Fig. 7. MNK1 is prerequisite for BPXV replication. ***(a) siRNA knockdown of MNK1:*** HeLa cells were transfected with control or MNK1 siRNA. At 48 h post-transfection, cells were infected with BPXV at MOI of 1 and virus yield in the infected cell culture supernatant was quantified by plaque assay. ***(b) Cytotoxicity of FR180204 (ERK inhibitor):*** Indicated concentrations of FR180204 or equivalent volumes of DMSO were incubated with cultured Vero cells for 96 h and cell viability (% survival) was measured by MTT assay. ***(c) Antiviral efficacy of ERK inhibitor:*** Vero cells were infected with BPXV for 1 h followed by washing with PBS and addition of fresh MEM containing either FR180204 (1 µg/ml) or 0.05% DMSO. Infectious virus released in the supernatant at 48 hpi was quantified by plaque assay. Error bars indicate SD. Pair-wise statistical comparisons were performed using Student's *t*-test (*** = P < 0.001, ** = P < 0.01).

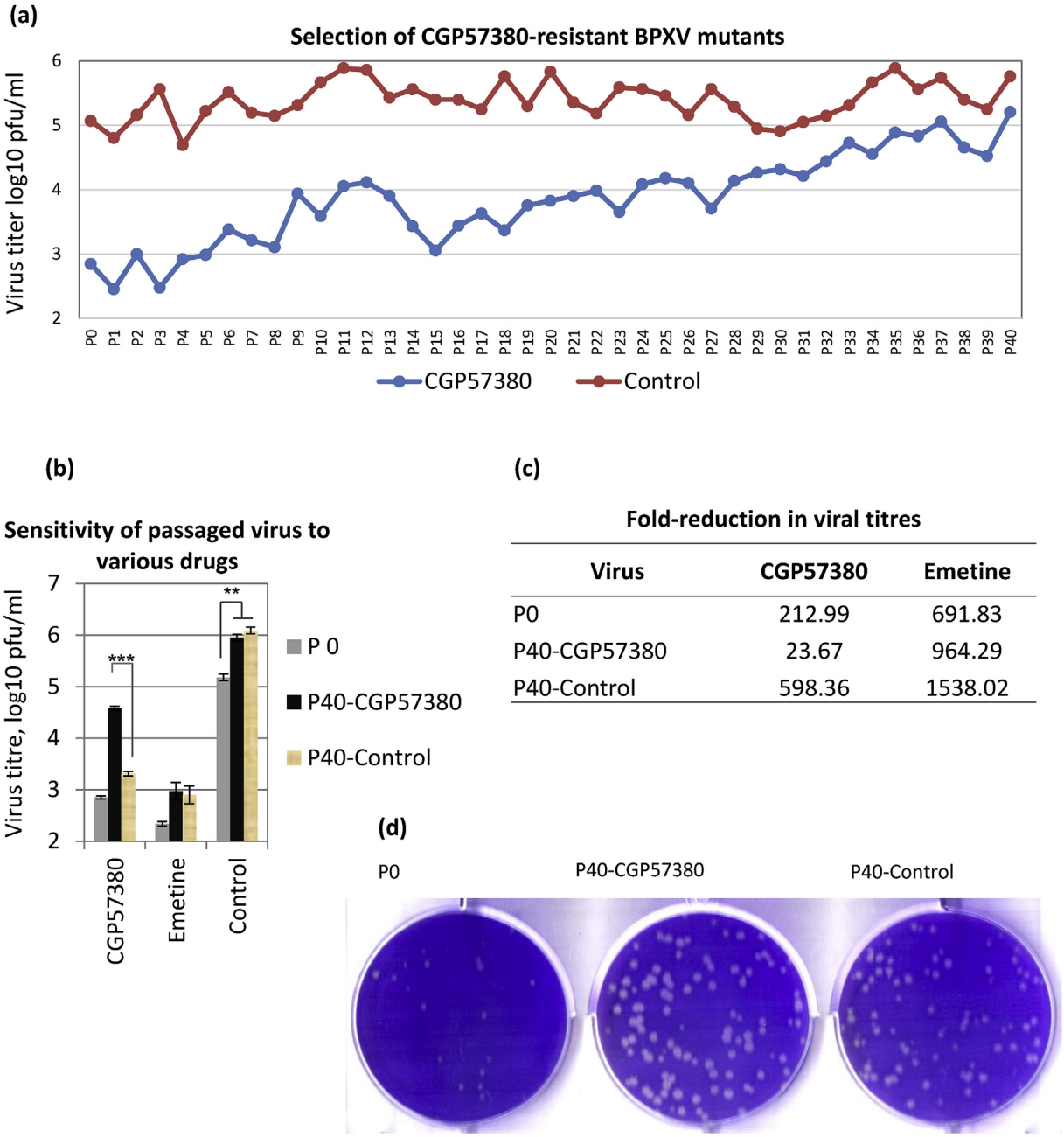

Virus	CGP57380	Emetine
P0	212.99	691.83
P40-CGP57380	23.67	964.29
P40-Control	598.36	1538.02

Fig. 8. Selection of CGP57380-resistant BPXV mutants. BPXV was sequentially passaged in Vero cells in the presence of 0.5 μg/ml CGP57380 or 0.05% DMSO. At each passage, confluent monolayers of Vero cells were infected with the virus, washed 5 times with PBS before a fresh aliquot of MEM was added and incubated for 48–96 h or until the appearance of cytopathic effect (CPE) in ≥75% cells. The virus released in the supernatant was termed as passage 1 (P1) and used in the second round of infection, which was termed as passage 2 (P2). Forty passages of virus infection were similarly carried out **(a).** At P40, in order to study the relative resistance against CGP57380, P0, P40-CGP57380 and P40-control viruses were used to infect Vero cells at MOI = 0.1 and grown in presence of either 0.05% DMSO or 1.5 μg/ml CGP57380. The virus yields in the infected cell culture supernatant were quantified by plaque assay **(b).** Fold-inhibition in virus replication (P0, P40-control and P40-CGP57380) in the presence of indicated drugs is shown **(c).** Plaque morphology of P0, P40-Control and P40-CGP57380 viruses is also shown **(d).**

compound previously known to exert anti-BPXV efficacy (Khandelwal et al., 2017). In contrast to the CGP57380-treated cells, the magnitude of viral inhibition in emetine-treated cells was comparable among P0, P40-Control and P40-CGP57380 viruses (Fig. 8b) suggesting that the resistance acquired by P40-CGP57380 virus was specifically directed against CGP57380 and did not acquire general resistance against other antiviral agents.

3.7. In ovo antiviral efficacy of CGP57380 against BPXV

Previously we developed an egg infection model for BPXV (Khandelwal et al., 2017) where BPXV infection produced distinct visible lesions (pocks) on CAM of embryonated chicken eggs (Khandelwal et al., 2017). We used this model to analyze the *in ovo* antiviral efficacy of CGP57380 against BPXV. BPXV at a titer of < 100 pfu/ml did not produce any pock lesions on the CAM, though higher concentrations (> 100 pfu/ml) produced pock lesions. The EID_{50} was calculated as $10^{3.49}$ pfu/egg (Fig. 9a).

LD_{50} was determined by inoculating various doses of CGP57380 in SPF embryonated chicken eggs. As shown in Fig. 9b, mortality of the embryo was observed at CGP57380 concentration ≥100 μg/egg but not at 50 μg/egg. The LD_{50} was determined to be 69.51 μg/egg.

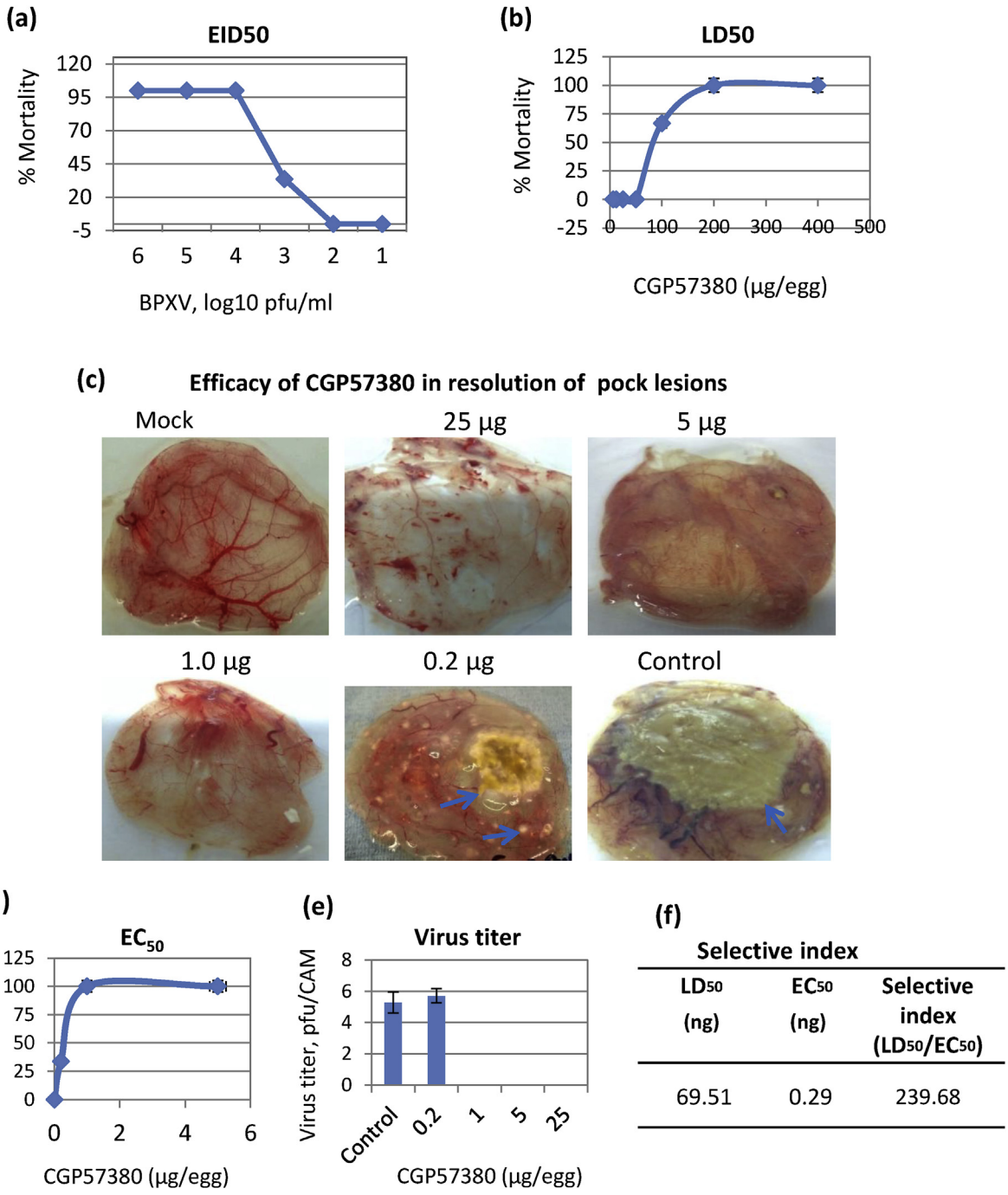

LD50 (ng)	EC50 (ng)	Selective index (LD50/EC50)
69.51	0.29	239.68

Fig. 9. ***In ovo*** **antiviral efficacy of CGP57380.** ***EID*****$_{50}$**: Embryonated SPF chicken eggs, in triplicates were infected via CAM route at indicated concentration of BPXV. At 5–7 dpi, eggs were examined for mortality and pock lesions on CAM. EID_{50} was determined by the Reed-Muench method **(a)**. ***LD*****$_{50}$**: Embryonated SPF chicken eggs, in triplicates, were inoculated with indicated concentration of CGP57380 via CAM route. At 5 days post-CGP57380 inoculation, eggs were visualized for the viability of embryos. LD_{50} was determined by the Reed-Muench method **(b)**. ***EC*****$_{50}$**: Embryonated SPF chicken eggs, in triplicate were inoculated with indicated concentration of CGP57380 along with BPXV infection at 100 EID_{50}. At 5 days post-CGP57380 inoculation, eggs were examined for mortality and pock lesions on CAM. BPXV-induced pock lesions on CAM and their resolution by CGP57380 are shown (**c**). EC_{50} was determined by Reed-Muench method **(d).** BPXV titers at various drug-regimens (**e**) and selective index (**f**) are also shown.

For evaluation of anti-BPXV efficacy of CGP57380, eggs were infected with BPXV at 100 EID_{50} along with various doses (25–0.2 µg/egg) of CGP57380. As shown in Fig. 9c, as compared to the vehicle-control, no obvious pock lesions (Fig. 9c) were observed at CGP57380 concentration ≥1 µg/egg. However, at lower concentration (≤0.2 µg/egg) CGP57380 could not prevent development of the pock lesions on CAM (Fig. 9c) as well as death of the embryos (Fig. 9d). The EC_{50} was determined to be 0.29 ng/egg. Besides protection against BPXV challenge, CGP57380-treated eggs also showed significantly reduced viral titres (Fig. 9e). Taken together, it was concluded that CGP57380 could provide protection against BPXV challenge infection in embryonated chicken eggs. The therapeutic index (LD_{50}/EC_{50}) was determined to be 239.68 (Fig. 9f).

4. Discussion

Host-targeting antiviral agents are less prone to develop drug resistant virus mutants and could have a significant impact on multiple virus genotypes (strain/serotype) to provide broad spectrum inhibition against different families of viruses (Conteduca et al., 2014; Khandelwal et al., 2017; Pawlotsky, 2012; Ruiz and Russell, 2012; Shahidi et al., 2014). This novel approach has led to the development of some promising compounds for treatment of HCV and HIV (Gilliam et al., 2011; von Hahn et al., 2011). By screening a library of kinase and phosphatase inhibitors, we identified MNK1 inhibitor CGP57380 as one of the candidate that blocked BPXV replication. MNK1 is one of the MAPKs activated kinase, expressed by all adult tissues except brain (Waskiewicz et al., 1997) and is mainly activated by ERK1/2 (Hargett et al., 2005; Roth et al., 2017). Its major downstream targets include eIF4E/4G, PSF [polypyrimidine tract binding (PTB)-associated splicing factor], heterogenous nuclear ribonucleoprotein A 1(hnRNPA1) and mTOR1. eIF4E/4G are involved in initiation of cap-dependent mRNA translation whereas mTOR1 is involved in regulating cap-independent translation. PSF and hnRNPA1 are associated with translocation and processing of mRNA (Kumar et al., 2018b).

Since virucidal effect was not observed on extracellular virus even at 40 μg/ml of CGP57380 (~25-fold higher than highest noncytotoxic concentration), the antiviral efficacy of CGP57380 is mediated via inhibition of the BPXV replication cycle in infected cells, rather than directly inactivating virion particles. In order to dissect specific step(s) of BPXV life cycle regulated by MNK1, we carried out time-of-addition and virus step-specific assays. Time-of-addition assay indicated involvement of MNK1 in regulation of the middle steps (post-entry) of BPXV life cycle. In virus step-specific assays, no effect of CGP57380 was observed on virus attachment, entry and budding. CGP57380 treatment specifically resulted in decreased synthesis of viral genome. Reduced synthesis of viral genome may eventually reflect decrease amount of viral proteins which we observed in Western blot analysis. Conversely, it is possible that the inhibitor treatment could have results in defective synthesis of viral proteins (viral polymerase) which would have eventually resulted in decreased synthesis of viral genome.

Viruses completely depend on the host translational machinery for synthesis of the viral proteins (Kumar et al., 2018a; Walsh and Mohr, 2004). Viral mRNAs may have a range of structures at its 5′ end. It may be capped with m7G or linked with viral genome-linked proteins (VPg). Uncapped viral mRNAs may carry *cis*-acting regulatory elements (CREs) such as internal ribosomal entry site (IRES) and protein binding sites. These 5′ end structures have been shown to regulate viral mRNA translation (Brown et al., 2014). MNK1 is involved in regulating both IRES- and cap-dependent viral mRNA translation (Kumar et al., 2018b).

Viral mRNA translation in most of the DNA viruses (including poxviruses) and some RNA viruses is synthesized in cap-dependent manner where eIF4E/eIF4G interaction plays a central role in translation initiation (Kumar et al., 2018b). Activated MNK1 directly binds to eIF4G in the initiation complex and phosphorylate eIF4E which subsequently binds to 5′ cap of mRNA to initiate translation (Kumar et al., 2018b). Depletion of MNK1 by small interfering RNA (siRNA), blocking activation of extracellular regulated kinase (ERK, an upstream activator of MNK1) and disruption of eIF4E/eIF4G interaction (downstream substrate for MNK1), resulted in reduced BPXV replication (Fig. 10), suggesting that ERK/MNK1/eIF4E signaling is prerequisite for BPXV replication. Disruption of ERK/MNK1/eIF4E signaling resulted in reduced synthesis of viral proteins, which confirmed that BPXV utilizes cap-dependent mechanism of translation initiation. Therefore we concluded that decreased synthesis of viral genome in presence of MNK1 inhibitor is the result of reduced synthesis of viral proteins.

The evidences of involvement of MNK1 in directly regulating viral genome synthesis are rare and seems to be associated with RNA viruses (Liu et al., 2009; Pathak et al., 2012; Wang and Zhang, 1999). In repeated attempts, we could not observe any direct interaction between MNK1 and BPXV genome (in infected cells) in chromatin immunoprecipitation (CHIP) assay (data not shown), which further supported our hypothesis that decreased synthesis of viral genome in presence of CGP57380 might be exclusively due to reduced synthesis of viral proteins.

In our study, peak MNK1 activation was observed during the middle stages (6 hpi-18 hpi) of viral replication cycle, time point when BPXV presumably synthesizes its genome/protein in the infected cells (Khandelwal et al., 2017). Therefore, it seems that BPXV exploits enhanced MNK1 signaling for optimal synthesis of its proteins.

Viruses rapidly develop drug-resistant variants, therefore, developing antiviral therapeutics is a major challenge (Chaudhary et al., 2015; Kumar et al., 2011, 2014; Pawlotsky, 2012). Whereas directly-acting antiviral agents are known to induce a completely resistant phenotype as early as at 6th passage (Kumar et al., 2011), no CGP57380-resistant BPXV variants were observed up to P20, suggesting that resistance to CGP57380 is unlikely to occur. There are also reports describing reduced tendency of host-targeting agents in inducing antiviral drug resistance on long-term *in vitro* culture (Kumar et al., 2011). However, on further higher passage (P40), we observed a significant resistance to CGP57380 in P40-CGP57380 virus, as compared to P40-control virus. P40-control virus did not exhibit any significant resistance against CGP57380 suggesting that resistance against CGP57380 is not a general phenomenon due to sequential high passages but rather a specific event acquired in presence of CGP57380. In a recent study (van der Schaar et al., 2012), Schaar and colleagues identified coxsackievirus B3 (CVB3) mutants that replicate efficiently in the presence of several potent antiviral drugs known to inhibit phosphatidylinositol-4-kinase IIIα (PI4KIIIα), a key cellular factor for CVB3 replication. The authors observed that a single point mutation in the viral 3A protein confers resistance and the drug resistant escape mutants of CVB3 could replicate in cells with low PI4KIIIα. Additionally, cyclosporine A resistant hepatitis C virus (HCV) mutant has also been identified (Chatterji et al., 2010; Coelmont et al., 2009). In our study, resistance acquired by BPXV against MNK1 inhibitor adds another example to a short list of viruses (Chatterji et al., 2010; Coelmont et al., 2009) that acquired resistance against a host-targeting antiviral agent. To become resistant against a host-targeting antiviral agent, virus may either switch to use an alternate host factor or may acquire an increased affinity to its substrate. Testing these hypotheses and mapping mutations in CGP57380-resistant BPXV variant would provide insights in understanding antiviral drug resistance against host-targeting agents, which needs further investigation.

By utilizing a previously developed BPXV egg infection model (Khandelwal et al., 2017), anti-BPXV efficacy of CGP57380 was also determined. A non-lethal dose of CGP57380 completely suppressed development of BPXV-induced pock lesions and associated mortality, as well as reduced viral titers in embryonated SPF eggs, suggesting its potential to be developed as a novel therapeutic agent. Since CGP57380 can inhibit cell metabolism, its long term use may eventually result in cytotoxicity. Therefore, its further validation, *in vivo* efficacy and clinical trials are required before actually introducing it from the research into the clinical settings.

In conclusion, MNK1 inhibitor exhibited a potent *in vitro* and *in ovo* antiviral efficacy against BPXV and was shown to impair synthesis of viral proteins. Host-targeting antiviral agents do not readily induce generation of drug resistant phenotypes, though at higher passage levels it may not be an unlikely event.

Acknowledgements

This work was supported by the Science and Engineering Research Board, Department of Science and Technology, Government of India [grant number SB/SO/AS-20/2014]. A part of this study belongs to MVSc thesis work of R. Kumar.

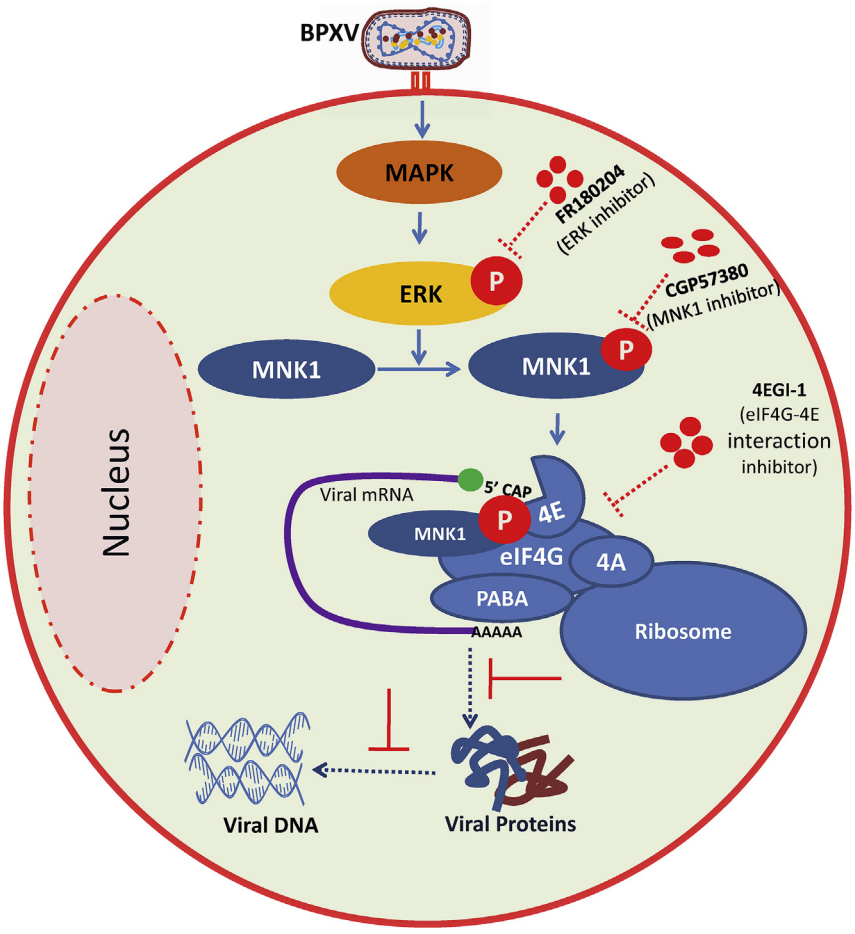

Fig. 10. ERK/MNK1/eIF4E signaling regulates synthesis of BPXV proteins. BPXV activates MNK1 signaling, mediated via MAPK/ERK pathway. Activated MNK1 induces phosphorylation of eIF4E that, in association with other translation initiation factors (eIF4E/eIF4G) regulates translation of viral proteins. Disruption of ERK/MNK1/eIF4E signaling results in reduced synthesis of viral proteins which eventually impedes synthesis of viral genome.

Appendix A. Supplementary data

Supplementary data to this article can be found online at https://doi.org/10.1016/j.antiviral.2018.10.022.

References

Andino, R., Domingo, E., 2015. Viral quasispecies. Virology 479–480, 46–51.

Bera, B., Shanmugasundaram, K., Barua, S., Anand, T., Riyesh, T., Vaid, R.K., Virmani, N., Bansal, M., Shukla, B.N., Malik, P., Singh, R.K., 2012. Sequence and phylogenetic analysis of host-range (E3L, K3L, and C7L) and structural protein (B5R) genes of buffalopox virus isolates from buffalo, cattle, and human in India. Virus Gene. 45, 488–498.

Boss, D.S., Beijnen, J.H., Schellens, J.H., 2009. Clinical experience with aurora kinase inhibitors: a review. Oncologist 14, 780–793.

Brown, M.C., Bryant, J.D., Dobrikova, E.Y., Shveygert, M., Bradrick, S.S., Chandramohan, V., Bigner, D.D., Gromeier, M., 2014. Induction of viral, 7-methyl-guanosine cap-independent translation and oncolysis by mitogen-activated protein kinase-interacting kinase-mediated effects on the serine/arginine-rich protein kinase. J. Virol. 88, 13135–13148.

Chatterji, U., Lim, P., Bobardt, M.D., Wieland, S., Cordek, D.G., Vuagniaux, G., Chisari, F., Cameron, C.E., Targett-Adams, P., Parkinson, T., Gallay, P.A., 2010. HCV resistance to cyclosporin A does not correlate with a resistance of the NS5A-cyclophilin A interaction to cyclophilin inhibitors. J. Hepatol. 53, 50–56.

Chaudhary, K., Chaubey, K.K., Singh, S.V., Kumar, N., 2015. Receptor tyrosine kinase signaling regulates replication of the peste des petits ruminants virus. Acta Virol. 59, 78–83.

Chen, Z.W., Hu, P., Ren, H., 2016. [A new challenge in clinical practice: resistance to directly acting antivirals in hepatitis C treatment]. Zhonghua Gan Zang Bing Za Zhi 24, 165–169.

Cinats, A., Heck, E., Robertson, L., 2018. Janus kinase inhibitors: a review of their emerging applications in dermatology. Skin Ther. Lett. 23, 5–9.

Coelmont, L., Kaptein, S., Paeshuyse, J., Vliegen, I., Dumont, J.M., Vuagniaux, G., Neyts, J., 2009. Debio 025, a cyclophilin binding molecule, is highly efficient in clearing hepatitis C virus (HCV) replicon-containing cells when used alone or in combination with specifically targeted antiviral therapy for HCV (STAT-C) inhibitors. Antimicrob. Agents Chemother. 53, 967–976.

Coito, C., Diamond, D.L., Neddermann, P., Korth, M.J., Katze, M.G., 2004. High-throughput screening of the yeast kinome: identification of human serine/threonine protein kinases that phosphorylate the hepatitis C virus NS5A protein. J. Virol. 78, 3502–3513.

Conteduca, V., Sansonno, D., Russi, S., Pavone, F., Dammacco, F., 2014. Therapy of chronic hepatitis C virus infection in the era of direct-acting and host-targeting antiviral agents. J. Infect. 68, 1–20.

Dumbell, K., Richardson, M., 1993. Virological investigations of specimens from buffaloes affected by buffalopox in Maharashtra State, India between 1985 and 1987. Arch. Virol. 128, 257–267.

Gilliam, B.L., Riedel, D.J., Redfield, R.R., 2011. Clinical use of CCR5 inhibitors in HIV and beyond. J. Transl. Med. 9 (Suppl. 1), S9.

Glover, K.Y., Perez-Soler, R., Papadimitradopoulou, V.A., 2004. A review of small-molecule epidermal growth factor receptor-specific tyrosine kinase inhibitors in development for non-small cell lung cancer. Semin. Oncol. 31, 83–92.

Goris, N., Vandenbussche, F., De Clercq, K., 2008. Potential of antiviral therapy and prophylaxis for controlling RNA viral infections of livestock. Antivir. Res. 78, 170–178.

Grzmil, M., Huber, R.M., Hess, D., Frank, S., Hynx, D., Moncayo, G., Klein, D., Merlo, A., Hemmings, B.A., 2014. MNK1 pathway activity maintains protein synthesis in rapalog-treated gliomas. J. Clin. Invest. 124, 742–754.

Gujarati, R., Reddy Karumuri, S.R., Babu, T.N., Janardhan, B., 2018. A case report of buffalopox: a zoonosis of concern. Indian J. Dermatol. Venereol. Leprol.

Gurav, Y.K., Raut, C.G., Yadav, P.D., Tandale, B.V., Sivaram, A., Pore, M.D., Basu, A., Mourya, D.T., Mishra, A.C., 2011. Buffalopox outbreak in humans and animals in Western Maharashtra, India. Prev. Vet. Med. 100, 242–247.

Hargett, D., McLean, T., Bachenheimer, S.L., 2005. Herpes simplex virus ICP27 activation of stress kinases JNK and p38. J. Virol. 79, 8348–8360.

Hartmann, J.T., Haap, M., Kopp, H.G., Lipp, H.P., 2009. Tyrosine kinase inhibitors - a review on pharmacology, metabolism and side effects. Curr. Drug Metabol. 10, 470–481.

Huang, X.B., Yang, C.M., Han, Q.M., Ye, X.J., Lei, W., Qian, W.B., 2018. MNK1 inhibitor CGP57380 overcomes mTOR inhibitor-induced activation of eIF4E: the mechanism of synergic killing of human T-ALL cells. Acta Pharmacol. Sin.

Khandelwal, N., Chander, Y., Rawat, K.D., Riyesh, T., Nishanth, C., Sharma, S., Jindal, N., Tripathi, B.N., Barua, S., Kumar, N., 2017. Emetine inhibits replication of RNA and DNA viruses without generating drug-resistant virus variants. Antivir. Res. 144, 196–204.

Knauf, U., Tschopp, C., Gram, H., 2001. Negative regulation of protein translation by mitogen-activated protein kinase-interacting kinases 1 and 2. Mol. Cell Biol. 21, 5500–5511.

Kumar, N., Barua, S., Riyesh, T., Chaubey, K.K., Rawat, K.D., Khandelwal, N., Mishra, A.K., Sharma, N., Chandel, S.S., Sharma, S., Singh, M.K., Sharma, D.K., Singh, S.V., Tripathi, B.N., 2016a. Complexities in Isolation and Purification of Multiple Viruses from Mixed Viral Infections: viral Interference, Persistence and Exclusion. PloS One 11, e0156110.

Kumar, N., Barua, S., Thachamvally, R., Tripathi, B.N., 2016b. Systems perspective of morbillivirus replication. J. Mol. Microbiol. Biotechnol. 26, 389–400.

Kumar, N., Maherchandani, S., Kashyap, S.K., Singh, S.V., Sharma, S., Chaubey, K.K., Ly, H., 2014. Peste des petits ruminants virus infection of small ruminants: a comprehensive review. Viruses 6, 2287–2327.

Kumar, N., Sharma, N.R., Ly, H., Parslow, T.G., Liang, Y., 2011. Receptor tyrosine kinase inhibitors that block replication of influenza a and other viruses. Antimicrob. Agents Chemother. 55, 5553–5559.

Kumar, N., Sharma, S., Barua, S., Tripathi, B.N., Rouse, B.T., 2018a. Virological and immunological outcomes of coinfections. Clin. Microbiol. Rev. 31.

Kumar, N., Xin, Z.T., Liang, Y., Ly, H., Liang, Y., 2008. NF-kappaB signaling differentially regulates influenza virus RNA synthesis. J. Virol. 82, 9880–9889.

Kumar, R., Khandelwal, N., Thachamvally, R., Tripathi, B.N., Barua, S., Kashyap, S.K., Maherchandani, S., Kumar, N., 2018b. Role of MAPK/MNK1 signaling in virus replication. Virus Res. 253, 48–61.

Lewis-Jones, S., 2004. Zoonotic poxvirus infections in humans. Curr. Opin. Infect. Dis. 17, 81–89.

Liu, Y., Wimmer, E., Paul, A.V., 2009. Cis-acting RNA elements in human and animal plus-strand RNA viruses. Biochim. Biophys. Acta 1789, 495–517.

Ludwig, S., Pleschka, S., Planz, O., Wolff, T., 2006. Ringing the alarm bells: signalling and apoptosis in influenza virus infected cells. Cell Microbiol. 8, 375–386.

Marinaik, C.B., Venkatesha, M.D., Gomes, A.R., Reddy, P., Nandini, P., Byregowda, S.M., 2018. Isolation and molecular characterization of zoonotic Buffalopox virus from skin lesions of humans in India. Int. J. Dermatol. 57, 590–592.

Martinez, A., Sese, M., Losa, J.H., Robichaud, N., Sonenberg, N., Aasen, T., Ramon, Y.C.S., 2015. Phosphorylation of eIF4E Confers Resistance to Cellular Stress and DNA-Damaging Agents through an Interaction with 4E-T: a Rationale for Novel Therapeutic Approaches. PloS One 10, e0123352.

Muhlbauer, D., Dzieciolowski, J., Hardt, M., Hocke, A., Schierhorn, K.L., Mostafa, A., Muller, C., Wisskirchen, C., Herold, S., Wolff, T., Ziebuhr, J., Pleschka, S., 2015. Influenza virus-induced caspase-dependent enlargement of nuclear pores promotes nuclear export of viral ribonucleoprotein complexes. J. Virol. 89, 6009–6021.

Nousiainen, L., Sillanpaa, M., Jiang, M., Thompson, J., Taipale, J., Julkunen, I., 2013. Human kinome analysis reveals novel kinases contributing to virus infection and retinoic-acid inducible gene I-induced type I and type III IFN gene expression. Innate Immun. 19, 516–530.

Pathak, K.B., Pogany, J., Xu, K., White, K.A., Nagy, P.D., 2012. Defining the roles of cis-acting RNA elements in tombusvirus replicase assembly in vitro. J. Virol. 86, 156–171.

Pawlotsky, J.M., 2012. The science of direct-acting antiviral and host-targeted agent therapy. Antivir. Ther. 17, 1109–1117.

Pleschka, S., Wolff, T., Ehrhardt, C., Hobom, G., Planz, O., Rapp, U.R., Ludwig, S., 2001. Influenza virus propagation is impaired by inhibition of the Raf/MEK/ERK signalling cascade. Nat. Cell Biol. 3, 301–305.

Riyesh, T., Karuppusamy, S., Bera, B.C., Barua, S., Virmani, N., Yadav, S., Vaid, R.K., Anand, T., Bansal, M., Malik, P., Pahuja, I., Singh, R.K., 2014. Laboratory-acquired buffalopox virus infection, India. Emerg. Infect. Dis. 20, 324–326.

Roth, H., Magg, V., Uch, F., Mutz, P., Klein, P., Haneke, K., Lohmann, V., Bartenschlager, R., Fackler, O.T., Locker, N., Stoecklin, G., Ruggieri, A., 2017. Flavivirus infection uncouples translation suppression from cellular stress responses. mBio 8.

Ruiz, A., Russell, S.J., 2012. A new paradigm in viral resistance. Cell Res. 22, 1515–1517.

Schoffski, P., Dumez, H., Clement, P., Hoeben, A., Prenen, H., Wolter, P., Joniau, S., Roskams, T., Van Poppel, H., 2006. Emerging role of tyrosine kinase inhibitors in the treatment of advanced renal cell cancer: a review. Ann. Oncol. 17, 1185–1196.

Shahidi, M., Tay, E.S., Read, S.A., Ramezani-Moghadam, M., Chayama, K., George, J., Douglas, M.W., 2014. Endocannabinoid CB1 antagonists inhibit hepatitis C virus production, providing a novel class of antiviral host-targeting agents. J. Gen. Virol. 95, 2468–2479.

Shveygert, M., Kaiser, C., Bradrick, S.S., Gromeier, M., 2010. Regulation of eukaryotic initiation factor 4E (eIF4E) phosphorylation by mitogen-activated protein kinase occurs through modulation of Mnk1-eIF4G interaction. Mol. Cell Biol. 30, 5160–5167.

Singh, R.K., Hosamani, M., Balamurugan, V., Bhanuprakash, V., Rasool, T.J., Yadav, M.P., 2007. Buffalopox: an emerging and re-emerging zoonosis. Anim. Health Res. Rev. 8, 105–114.

Singh, R.K., Hosamani, M., Balamurugan, V., Satheesh, C.C., Shingal, K.R., Tatwarti, S.B., Bambal, R.G., Ramteke, V., Yadav, M.P., 2006. An outbreak of buffalopox in buffalo (Bubalus bubalis) dairy herds in Aurangabad, India. Rev. Sci. Technol. 25, 981–987.

van der Schaar, H.M., van der Linden, L., Lanke, K.H., Strating, J.R., Purstinger, G., de Vries, E., de Haan, C.A., Neyts, J., van Kuppeveld, F.J., 2012. Coxsackievirus mutants that can bypass host factor PI4KIIIbeta and the need for high levels of PI4P lipids for replication. Cell Res. 22, 1576–1592.

Venkatesan, G., Balamurugan, V., Prabhu, M., Yogisharadhya, R., Bora, D.P., Gandhale, P.N., Sankar, M.S., Kulkarni, A.M., Singh, R.K., Bhanuprakash, V., 2010. Emerging and re-emerging zoonotic buffalopox infection: a severe outbreak in Kolhapur (Maharashtra), India. Vet. Ital. 46, 439–448.

von Hahn, T., Ciesek, S., Manns, M.P., 2011. Arrest all accessories–inhibition of hepatitis C virus by compounds that target host factors. Discov. Med. 12, 237–244.

Walsh, D., Mohr, I., 2004. Phosphorylation of eIF4E by Mnk-1 enhances HSV-1 translation and replication in quiescent cells. Genes Dev. 18, 660–672.

Wang, Q., Su, L., Liu, N., Zhang, L., Xu, W., Fang, H., 2011. Cyclin dependent kinase 1 inhibitors: a review of recent progress. Curr. Med. Chem. 18, 2025–2043.

Wang, Y., Zhang, X., 1999. The nucleocapsid protein of coronavirus mouse hepatitis virus interacts with the cellular heterogeneous nuclear ribonucleoprotein A1 in vitro and in vivo. Virology 265, 96–109.

Waskiewicz, A.J., Flynn, A., Proud, C.G., Cooper, J.A., 1997. Mitogen-activated protein kinases activate the serine/threonine kinases Mnk1 and Mnk2. EMBO J. 16, 1909–1920.